Preparation of Monodisperse Au/TiO_2 Nanocatalysts via Self-Assembly

Jing Li and Hua Chun Zeng*

Department of Chemical and Biomolecular Engineering, Faculty of Engineering, National University of Singapore, 10 Kent Ridge Crescent, Singapore 119260

Received February 14, 2006. Revised Manuscript Received June 29, 2006

In this work, we report that presynthesized metallic nanoparticles (such as gold nanoparticles), rather than on-site growing ones that are prepared under thermally or photochemically activated conditions, can be "impregnated" uniformly onto premade oxide supports with organic interconnects which have bifunctional groups. Methodic features of this general technique have been demonstrated using a model metal−oxide system, Au/TiO_2 (TiO_2 in anatase phase) catalyst, in the photodegradation of organic compounds (e.g., methyl orange). On the basis of our investigations with a range of analytical techniques, it has been further found that, if desired, permanent engagement and direct contact between the supported metals and oxide carriers can also be achieved with additional heat treatments. In principle, other oxide-supported metal catalysts can also be fabricated at low temperatures through these types of self-assembling routes.

Introduction

Conventional impregnation method for oxide-supported metal catalysts for heterogeneous catalysis involves a number of processing steps:[1,2] soaking the oxide carriers in a metal salt precursor solution, drying, thermal decomposition of precursor salt to surface oxide, and reduction of the surface oxide to metallic particles (i.e., active catalytic components). Because of uneven precursor-solution loading caused by gravitational settlement and trapping among the catalyst carriers, metal particles generated from this conventional process are normally polydispersed. Metal agglomeration, including chemical modification of support through (metal) ionic diffusion upon thermal treatments, is a major drawback for these kinds of methods. Furthermore, surface active sites, such as atomic and ionic defects and vacancies, atomic steps, kinks, and terraces, of both surface metals and oxide carriers are often diminished along these high-temperature treatments, as schematically illustrated in Figure 1a.

As a model system, catalysts of metal oxide-supported gold (Au) nanoparticles has been investigated extensively over the past 2 decades, due to their many important applications such as low-temperature oxidation of carbon monoxide.[3,4] Several attempts, with both gas and liquid techniques, have been made recently for supported nanosized Au/TiO_2.[3−10] Nonetheless, fabrication for highly monodispersed metal loading has so far remained unsuccessful. To further this research, we note that newer fabrication methods may be attainable by taking advantage of solution chemistry of metallic nanoparticles, which has become a very matured research field in recent years; numerous synthetic methods have been in place.[11−15] Herein, as depicted in Figure 1b, we report that monodispersed Au nanoparticles, 2−4 nm in size, can be presynthesized in solution and later assembled

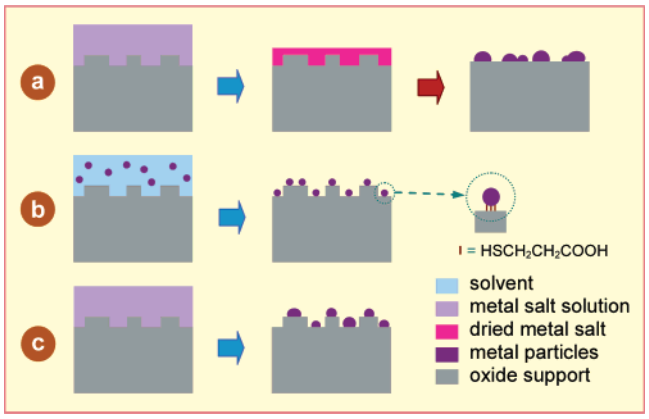

Figure 1. Illustrative comparison: (a) conventional metal ion impregnation method (oxide in precursor salt solution, drying, and thermal treatment (calcination and reduction)); (b) the present "impregnation" method (oxide in metal suspension and drying); and (c) photoassisted reductive method (oxide in precursor salt solution and photocatalytic reduction of metal cations, another soft method studied in this work).

* To whom correspondence should be addressed. E-mail: chezhc@nus.edu.sg.

(1) Stiles, A. B.; Koch, T. A. *Catalyst Manufacture*, 2nd ed.; Dekker: New York, 1995.
(2) Zeng, H. C. In *The Dekker Encyclopedia of Nanoscience and Nanotechnology*; Dekker: New York, 2004; pp 2539−2550.
(3) Haruta, M. *Catal. Today* **1997**, *36*, 153−166.
(4) Valden, M.; Lai, X.; Goodman, D. W. *Science* **1998**, *281*, 1647−1650.
(5) Chou, J.; McFarland, E. W. *Chem. Commun. (Cambridge)* **2004**, 1648−1649.
(6) Li, D.; McCann, J. T.; Gratt, M.; Xia, Y. N. *Chem. Phys. Lett.* **2004**, *394*, 387−391.
(7) Tada, H.; Soejima, T.; Ito, S.; Kobayashi, H. *J. Am. Chem. Soc.* **2004**, *126*, 15952−15953.
(8) (a) Yan, W. F.; Mahurin, S. M.; Pan, Z. W.; Overbury, S. H.; Dai, S. *J. Am. Chem. Soc.* **2005**, *127*, 10480−10481. (b) Tian, Y.; Tatsuma, T. *J. Am. Chem. Soc.* **2005**, *127*, 7632−7637.
(9) (a) Tong, X.; Benz, L.; Kemper, P.; Metiu, H.; Bowers, M. T.; Buratto, S. K. *J. Am. Chem. Soc.* **2005**, *127*, 13516−13518. (b) Remediakis I. N.; Lopez, N.; Nørskov, J. K. *Angew. Chem., Int. Ed.* **2005**, *44*, 1824−1826. (c) Yoon, B.; Häkkinen, H.; Landman, U. *J. Phys. Chem. A* **2003**, *107*, 4066−4071.
(10) Li, J.; Zeng, H. C. *Angew. Chem., Int. Ed.* **2005**, *44*, 4342−4345.
(11) Brust, M.; Walker, M.; Bethell, D.; Schiffrin, D. J.; Whyman, R. *J. Chem. Soc., Chem. Commun.* **1994**, 801−802.

10.1021/cm060362r CCC: $33.50
Published on Web 08/05/2006

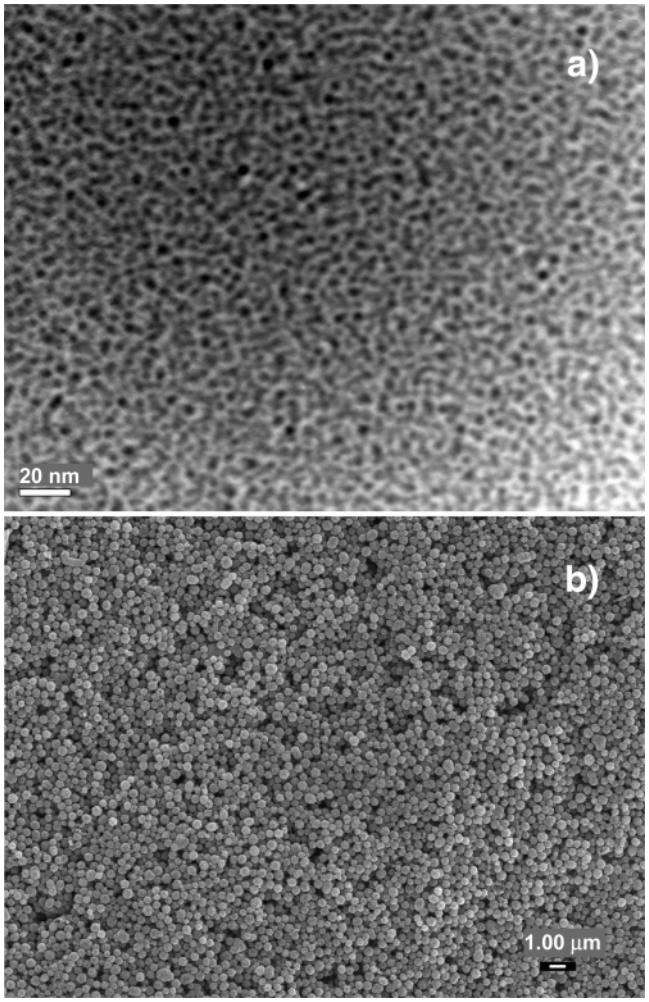

Figure 2. Overall views of samples: (a) TEM image for starting Au nanoparticles and (b) FESEM image of resultant Au/TiO_2 catalyst prepared by the route b of Figure 1, which takes a spherical shape.

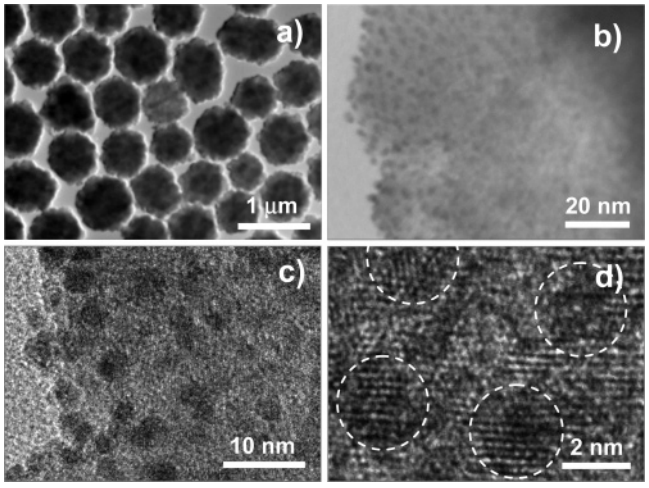

Figure 3. TEM images of as-prepared Au/TiO_2: (a) Au-loaded TiO_2 spheres (route b, Figure 1) and (b) 2−4 nm Au particles on the TiO_2 surface. HRTEM images of Au/TiO_2 after 30 min of reaction (also see Figure 4): (c) Au particle distribution and (d) individual Au particles and their lattice fringes.

evenly onto anatase TiO_2 support at low temperature. The prepared Au/TiO_2 catalyst has also been tested for organic compound degradation,[16] and an excellent photocatalytic activity has been demonstrated.

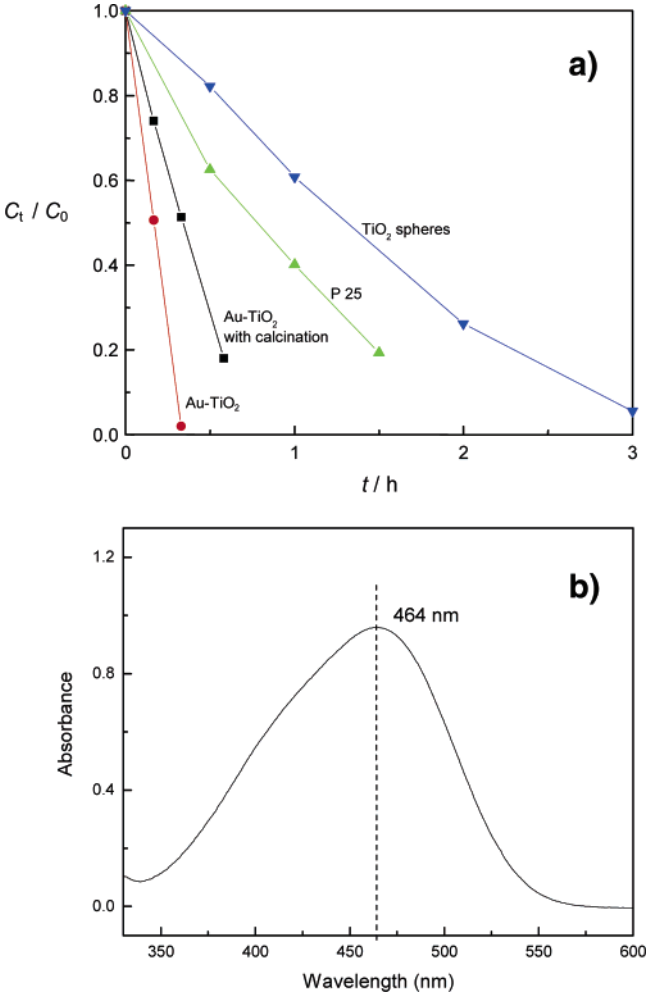

Figure 4. (a) Photocatalytic conversions of methyl orange using the Au/TiO_2 catalysts prepared in this work and referenced TiO_2 catalysts (see the text) and (b) a representative UV absorption spectrum of methyl orange used in the concentration determination of a. Experimental conditions: 10 mg of Au/TiO_2 or 10 mg of TiO_2 catalyst and 4.0 mL of methyl orange (C_0 = 10 mg/L) under UV irradiation (see Experimental Section).

Experimental Section

In synthesis of Au nanoparticle suspension, tetra-*n*-octylammonium bromide ($[CH_3(CH_2)_7]_4NBr$, TOAB; 0.19 g in 7.0 mL of toluene) and $HAuCl_4$ (12 mL, 0.01 M in water) were vigorously stirred in order to transfer $HAuCl_4$ to toluene phase, followed by adding 1.0 mL of 0.22 M dodecanethiol ($CH_3(CH_2)_{11}SH$, DDT) in toluene. Afterward, 12.0 mL of freshly prepared 0.1 M $NaBH_4$ aqueous solution was added to obtain 2−4 nm Au particles (transmission electron microscopy (TEM) image, Figure 2).[11] Spherical TiO_2 support in anatase polymorph was obtained by hydrolyzing 30.0 mL of 2.67 mM TiF_4 at 180 °C for 2 h, followed by a similar postgrowth treatment described in the literature.[17] The

(12) Kanehara, M.; Oumi, Y.; Sano, T.; Teranishi, T. *J. Am. Chem. Soc.* **2003**, *125*, 8708−8709.
(13) Maye, M. M.; Luo, J.; Lim, I. S.; Han, L.; Kariuki, N. N.; Rabinovich, D.; Liu, T. B.; Zhong, C.-J. *J. Am. Chem. Soc.* **2003**, *125*, 9906−9907.
(14) Hao, E.; Bailey, R. C.; Schatz, G. C.; Hupp, J. T.; Li, S. Y. *Nano Lett.* **2004**, *4*, 327−330.
(15) (a) Subramanian, V.; Wolf, E. E.; Kamat, P. V. *J. Am. Chem. Soc.* **2004**, *126*, 4930−4950. (b) Ojamäe, L.; Aulin, C.; Pedersen, H.; Käll, P.-O. *J. Colloid Interface Sci.* **2006**, *296*, 71−78.
(16) Carp, O.; Huisman, C. L.; Reller, A. *Prog. Solid State Chem.* **2004**, *32*, 33−177.
(17) Yang, H. G.; Zeng, H. C. *J. Phys. Chem. B* **2004**, *108*, 3492−3495.

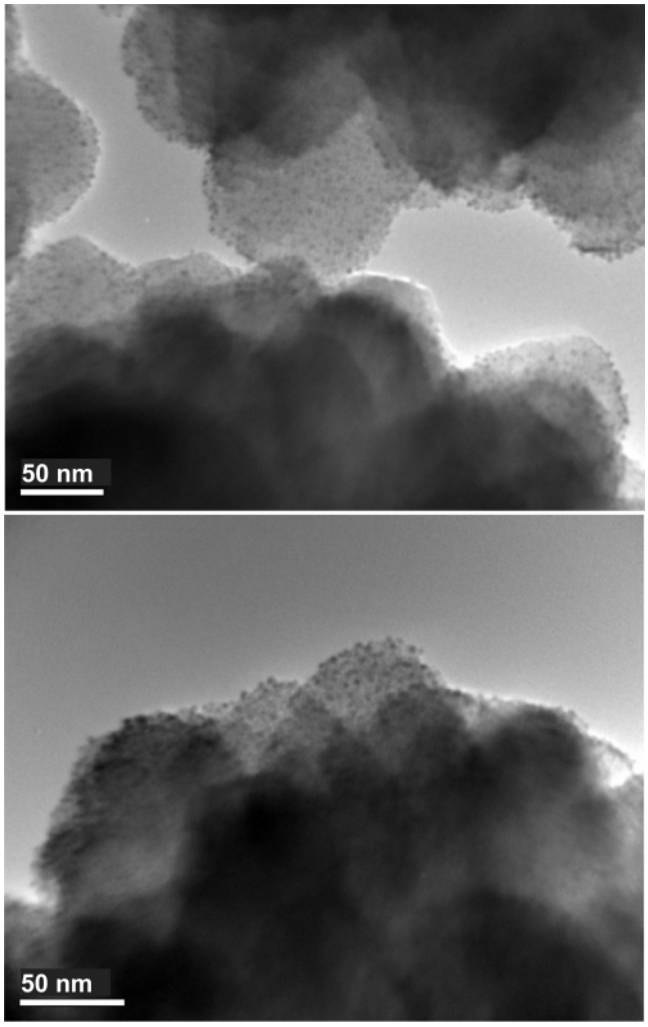

Figure 5. TEM images indicating that the anchored Au nanoparticles (2−4 nm) are still stabilized after a prolonged UV irradiation. Experimental conditions: 10 mg of Au/TiO_2 catalyst and 4.0 mL of methyl orange (C_0 = 10 mg/L) under UV irradiation for 9 h.

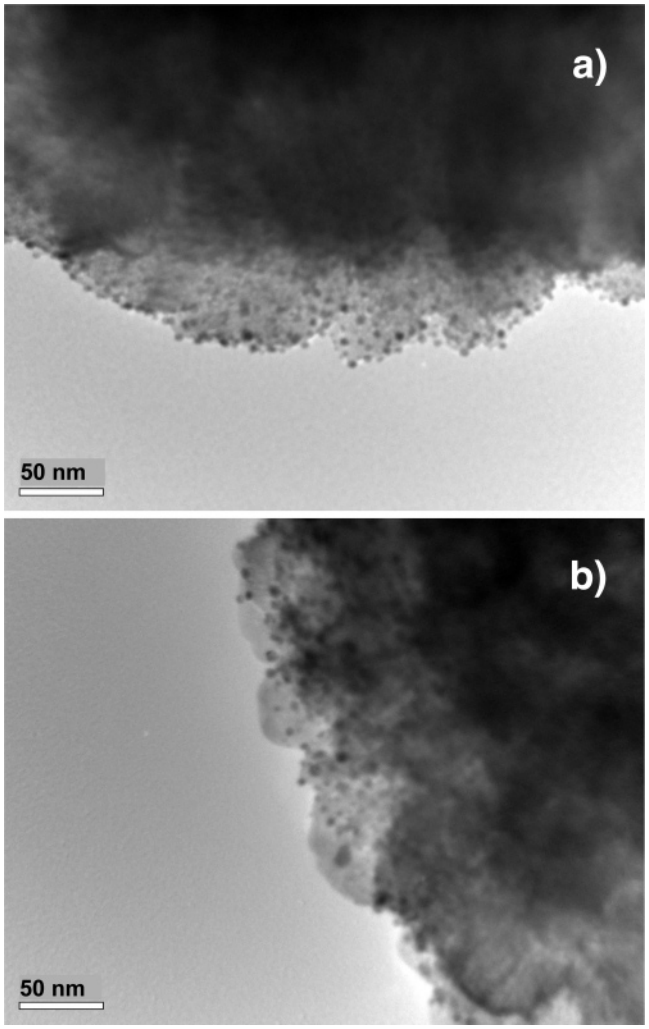

Figure 6. TEM images of heat-treated and used Au/TiO_2 catalysts: (a) heat-treated catalyst (300 °C for 3 h) and (b) catalyst a used after photoreactions for 9 h.

prepared TiO_2 spheres (20.0 mg) were then mixed with a 3-mercaptopropionic acid solution ($HS(CH_2)_2COOH$, MPA; 1.0 mL, 0.22 M in toluene), and the mixture was sonicated in an ultrasonic water bath for 10 min, after which 0.5 mL of the Au suspension was added and sonicated for another 10 min. Continuously aging for 3 h, the prepared Au/TiO_2 catalyst was washed with acetone for 3 times and dried at 60 °C overnight (field emission scanning electron microscopy (FESEM) image, Figure 3). The resultant catalyst showed a gray color. In photocatalytic testing, a dilute methyl orange aqueous solution (10 mg/L) was first bubbled with air for 1 h; then 10 mg of the Au/TiO_2 catalyst was dispersed in 4.0 mL of the above solution in a glass reactor and sonicated for 10 min. The reactor was rotated on a rolling station under a UV lamp (UVP R-52G, 254 nm, 2400 $\mu W/cm^2$). After each reaction, the solution was separated from catalyst by centrifugation. The concentration of methyl orange was measured with a UV−vis−near-IR scanning spectrophotometer (Shimadzu UV-3101PC). The crystallographic structure of the solid samples was determined with X-ray diffraction (XRD, Shimadzu XRD-6000, Cu Kα). The spatial, morphological, and compositional studies were carried out with field-emission scanning electron microscopy and energy-dispersive X-ray spectroscopy (FESEM/EDX; JSM-6700F), transmission electron microscopy (TEM, JEM-2010F; HRTEM, Tecnai-G^2, FEI), and Fourier transform infrared spectroscopy (FTIR, KBr pellet method, Bio-Rad FTS 135). Furthermore, X-ray photoelectron spectroscopy (XPS, AXIS-Hsi, Kratos Analytical) was used to investigate the compositional evolutions of used and treated catalyst surface. The spectra of all interested elements were referenced to the C 1s peak arising from adventitious carbon (binding energy (BE) was set at 284.6 eV).[10]

Results and Discussion

In our general materials characterization, crystallographic phases and chemical compositions of all prepared catalyst samples reported in this work were confirmed routinely with XRD, EDX, and XPS, as we did in the previous studies.[10,17,18] It should be noted that there are actually two tiers of self-organization in this catalyst fabrication. The first tier, the spherical self-aggregation of anatase TiO_2 nanocrystallites, has been detailed in our previous report.[17] The second tier, introduction of gold nanoparticles onto the above-prepared TiO_2 support, will be the main focus of the present study. In Figure 2a, presynthesized gold nanoparticles were first investigated with TEM to ensure their size uniformity. Figure 2b shows the general morphology of an Au/TiO_2 catalyst prepared by the present self-assembly method (Figure 1b).

(18) Shon, Y.-S.; Gross, S. M.; Dawson, B.; Porter, M.; Murray, R. W. *Langmuir* **2000**, *16*, 6555−6561.

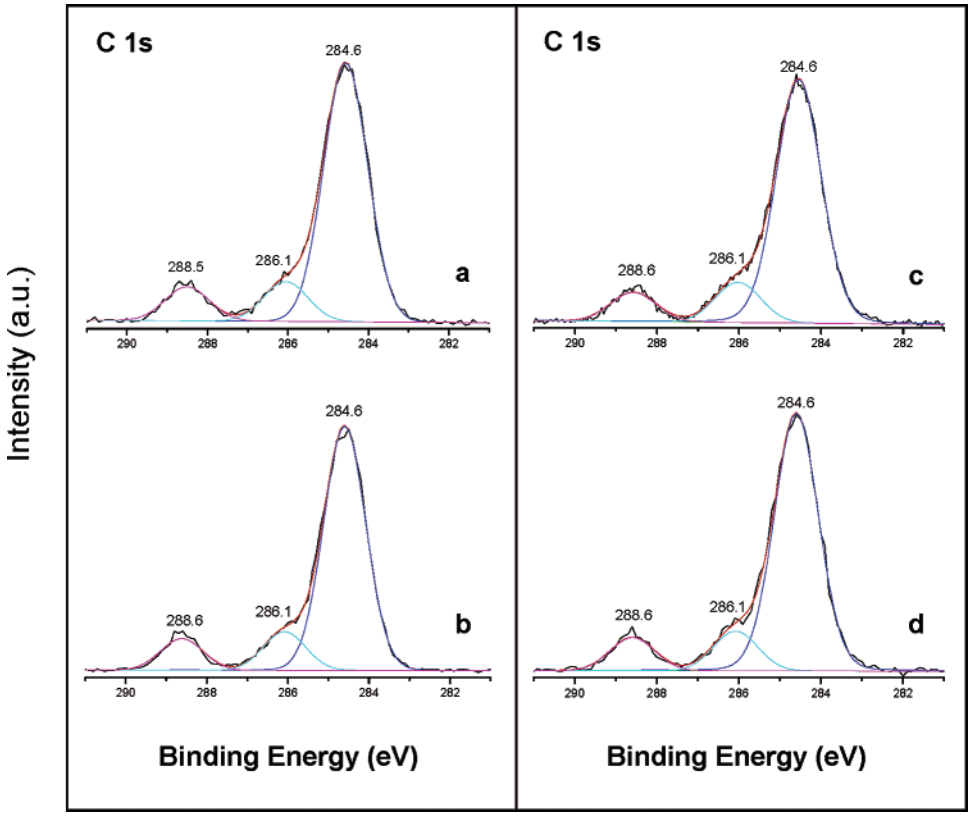

Figure 7. XPS spectra of C 1s: (a) as-prepared Au/TiO$_2$ catalysts, (b) the catalyst in a used after photoreactions for 9 h, (c) heat-treated Au/TiO$_2$ catalyst (300 °C for 3 h), and (d) the catalyst in c used after photoreactions for 9 h.

The Au metal loading can be controlled in a range of about 1−5 wt % (see Supporting Information). Indeed, both the presynthesized Au nanoparticles and TiO$_2$ nanospheres (and therefore their resultant Au/TiO$_2$ catalyst) are highly monodispersed. Quite surprisingly, as displayed in Figure 3, Au nanoparticles with small sizes of only 3.64 ± 0.70 nm can be distributed extremely evenly across an entire surface of TiO$_2$ nanosphere carrier (500−800 nm in diameter, Figure 3b,c) for the first time with this self-organizing method. Furthermore, most metal nanoparticles are discrete, separated with an interparticle distance of 2−6 nm, and the crystallinity of Au nanoparticles and the spherical TiO$_2$ support are also clearly shown in their lattice fringes (Figure 3d).[8,13]

The achieved uniformity of metal particle distribution can be primarily attributed to the presence of bifunctional groups in the MPA linker molecules. The interconnectivity of MPA molecules to Au and TiO$_2$ nanoparticles (i.e., Au and TiO$_2$ both in comparable sizes) has been investigated,[15] where the carboxyl end of MPA is adsorbed on the metal oxide surface while its thiol tail, on the metal. In this agreement, it was indeed observed in our experiments that the Au suspension becomes less colorful when they are introduced to the MPA-adsorbed TiO$_2$ nanospheres. In view of the assembling nature of this process, it is further anticipated that with this method the dimension and population of metal nanoparticles on the oxide support can be controlled precisely, because the size and amount of metal nanoparticles allocated can be predetermined in a catalyst preparation. Apparently, the self-assembling feature of the present method is rather unique, concerning a progressive paradigm shift of catalyst design and fabrication to "bottom-up" approaches.

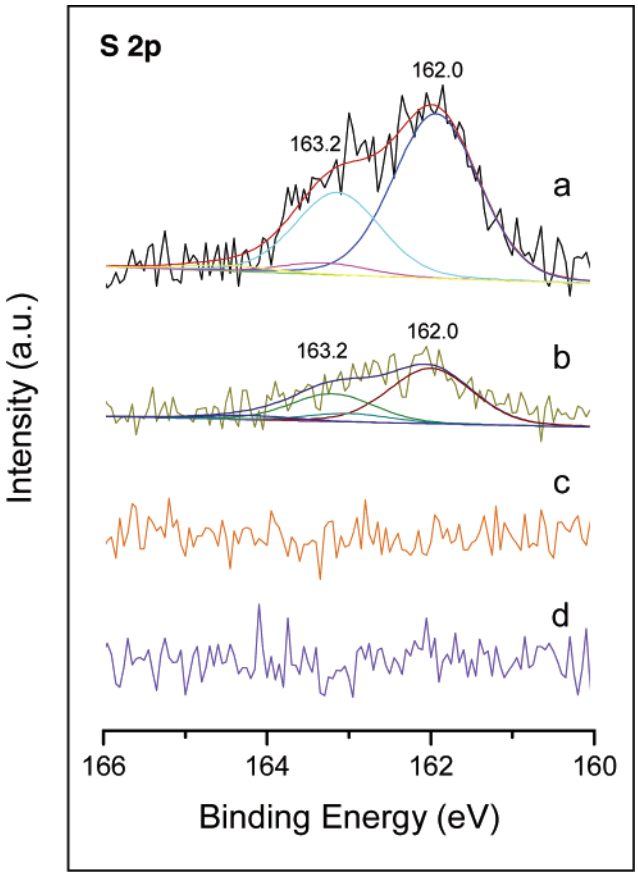

Figure 8. XPS spectra of S 2p: (a) as-prepared Au/TiO$_2$ catalysts, (b) the catalyst in a used after photoreactions for 9 h, (c) heat-treated Au/TiO$_2$ catalyst (300 °C for 3 h), and (d) the catalyst in c used after photoreactions for 9 h.

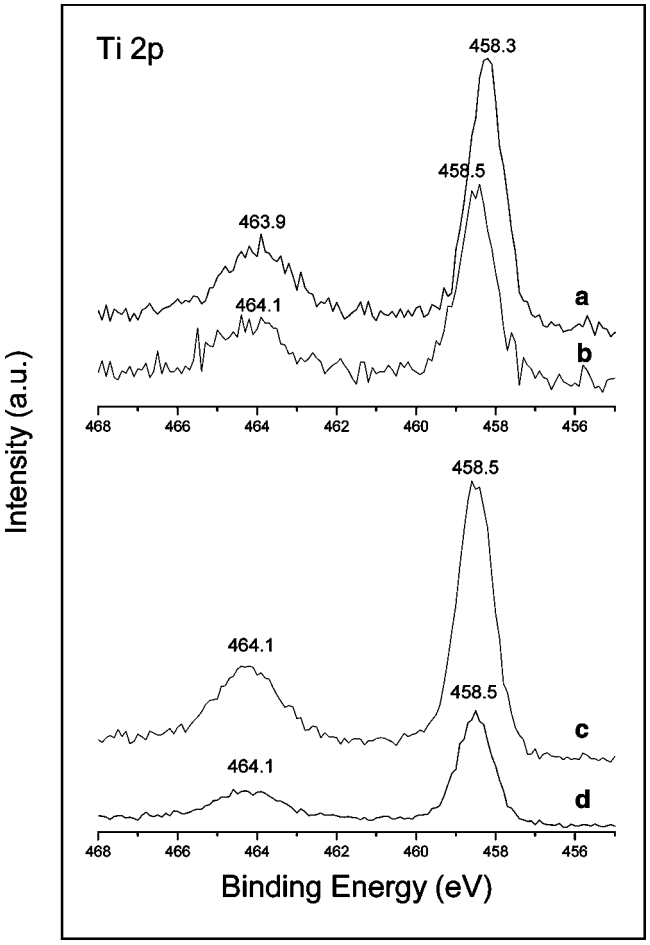

Figure 9. XPS spectra of Ti 2p: (a) as-prepared Au/TiO_2 catalysts, (b) the catalyst in a used after photoreactions for 9 h, (c) heat-treated Au/TiO_2 catalyst (300 °C for 3 h), and (d) the catalyst in c used after photoreactions for 9 h.

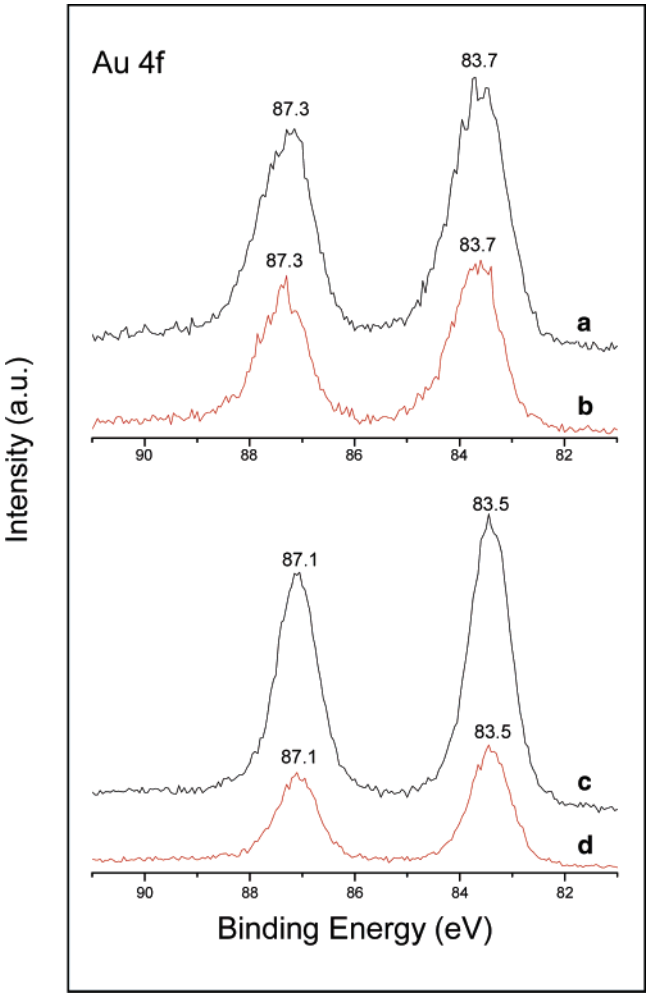

Figure 10. XPS spectra of Au 4f: (a) as-prepared Au/TiO_2 catalysts, (b) the catalyst in a used after photoreactions for 9 h, (c) heat-treated Au/TiO_2 catalyst (300 °C for 3 h), and (d) the catalyst in c used after photoreactions for 9 h.

To evaluate the activity of Au/TiO_2 catalyst under a real working environment, we compared a range of TiO_2 catalysts in photodegradation of methyl orange. The photocatalytic activities of the studied catalysts are reported in Figure 4a, on the basis of measuring a strong absorption band of methyl orange at 464 nm (Figure 4b). As can be seen, a significant decrease in the C_t/C_0 ratio (where C_0 is the initial concentration of methyl orange and C_t is the concentration of methyl orange left at time t) can be attained with the addition of Au nanoparticles onto the TiO_2 catalysts. Compared with the pure anatase TiO_2 nanospheres (which was used as the catalyst carrier in the present study; specific surface area, 40−45 m^2/g),[17] a significant reduction in the C_t/C_0 ratio is observed in the self-assembled Au/TiO_2. It is believed that the surface Au acts as local electron reservoirs and prevents recombination of photogenerated holes and electrons upon the irradiation of UV light,[15a] although the predissolved oxygen also functions as an electron receiver in the reactions. In addition to the above results, the self-assembled Au/TiO_2 catalyst also shows a rapid decrease in the C_t/C_0 ratio over a commercial TiO_2 catalyst (P 25, Degussa),[5] which has a similar specific surface area at 45−50 m^2/g but with mixed phases of rutile and anatase TiO_2. All these results show that the synergetic action between Au and TiO_2 is excellent in the catalysts prepared with the present method.

It is important to note that the UV irradiation and related photochemical reactions do not cause obvious metal coarsening. This observation has been reported in Figure 3c,d for a used catalyst. Quite encouragingly, as also shown in Figure 5, both the density and size of Au particles were not changed appreciably even with the prolonged UV irradiations. It is thus concluded that the anchored Au nanoparticles are indeed immobile on the TiO_2 surface under UV irradiation. Apparently, the small MPA interconnect used here can withstand the photoreactions imposed; a recent theoretical calculation reports that the adsorption energy of a carboxyl group on TiO_2 surfaces is about 150 kJ/mol.[15b] The process is also probably benefited from a short distance between Au and TiO_2 for photoelectron tunneling using this organic linker. Therefore, it seems that our low-temperature route for catalyst fabrication is feasible for a practical use. To further demonstrate methodic features of the present approach, the as-prepared Au/TiO_2 was heat-treated in air at 300 °C for 3 h. The catalyst morphology resulting from this process is reported in Figure 6, and the photocatalytic activity of this heat-treated sample is also given in Figure 4. In agreement with a small degree of aggregation of Au nanoparticles (i.e., growth; they became 4.48 ± 0.74 nm) at this moderate processing temperature, the catalytic activity of the heated

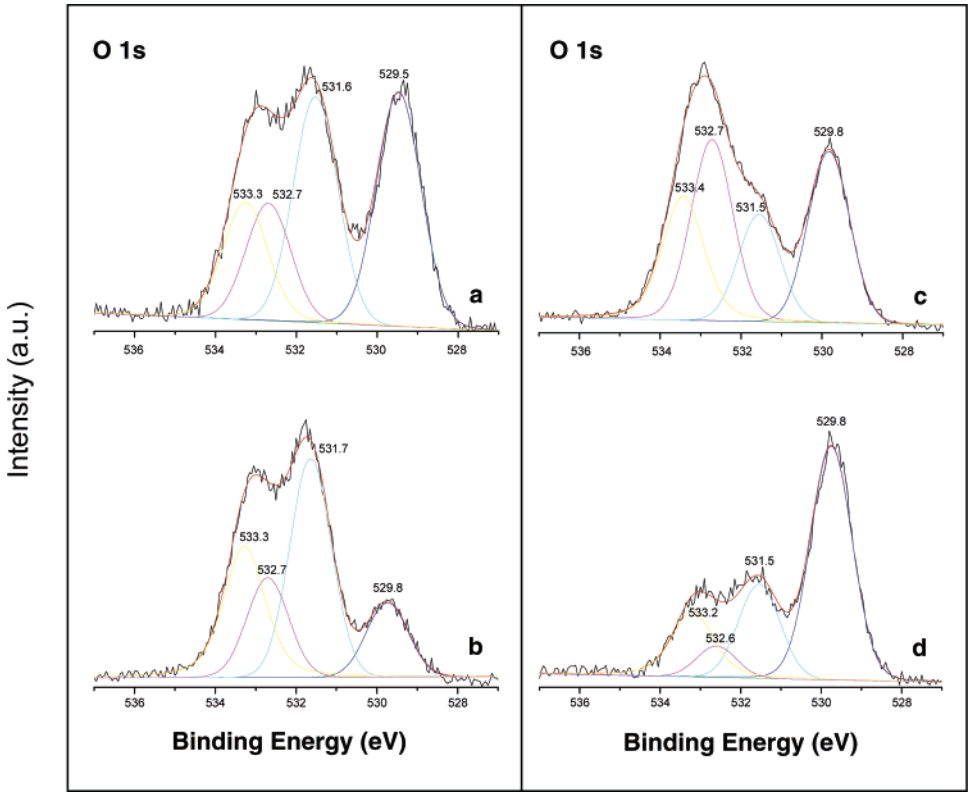

Figure 11. XPS spectra of O 1s: (a) as-prepared Au/TiO$_2$ catalysts, (b) the catalyst in a used after photoreactions for 9 h, (c) heat-treated Au/TiO$_2$ catalyst (300 °C for 3 h), and (d) the catalyst in c used after photoreactions for 9 h.

catalyst for the conversion of methyl orange is deteriorated (Figure 4). The heating seems to have also caused a population reduction of inherited structural defects of the pristine gold nanoparticles and the anatase support, which are believed to be catalytically more reactive.[2] This treatment, however, can generate a more permanent engagement or direct contact between the metal and support for the self-assembled type of catalysts in order to sustain harsher reacting environments, as required in "traditional" Au-based catalysts used for oxidation.[9] It is also recognized that despite the certain deterioration in catalytic activity, the heat-treated Au/TiO$_2$ is still a second most active catalyst in the present study (Figure 4). The *anchoring-then-heating* route developed here may serve as a new means for general fabrication of high-performance supported metal catalysts.

It is noted that the Au nanoparticles in the as-prepared Au/TiO$_2$ prior to thermal treatment or photoreactions are chemically bonded to both the surfactant DDT and bifunctional linker MPA. While the MPA molecules bind the Au nanoparticles to the TiO$_2$ support, the DDT keeps Au nanoparticles apart in the initial metal-particle suspensions as well as during their deposition process to the TiO$_2$ support. In particular, asymmetric and symmetric IR vibrational modes of C−H (CH_2) at 2920 and 2850 cm^{-1} and weaker modes of C−H (CH_3) at 2962 and 2878 cm^{-1} from DDT molecules can be observed simultaneously in the as-prepared Au/TiO$_2$ catalyst.[18] After photoreactions (Figure 4), it is found that the amount of S-containing surfactants was drastically reduced, due to a reductive desorption of anionic species from the Au surface.[7]

To have an in-depth understanding of the above process, surface composition of this catalyst system upon various reactions was further investigated by XPS method. The XPS spectra of C 1s in Figure 7 are nearly the same for all four samples. Three deconvoluted peaks are positioned at 284.6, 286.1, and 288.5−288.6 eV, respectively.[19] While it predominantly arises from adventitious carbon, the C 1s peak at 284.6 eV also includes the contribution from aliphatic hydrocarbon chains from surfactants (e.g., DDT, MPA, and TOAB for a and MPA for b).[19] The spectra also exhibit C−OH and/or C−O−C species at a BE of 286.1 eV, which can be ascribed to the oxidized carbon species of adventitious carbon as well as aliphatic hydrocarbons of the surfactants (catalysts a and b).[19] Compared to the heat-treated catalysts c and d, however, organic-containing samples a and b display no obvious advantage in the two peak areas (284.6 and 286.1 eV). It is because their surface contents are much lower than adventitious carbon. As commonly assigned, the peaks at 288.5−288.6 eV can be assigned to CO_3^{2-} from atmospheric CO_2 adsorption.[20]

In fitting the S $2p_{3/2}$ and S $2p_{1/2}$ doublet, as shown in Figure 8, a spin−orbit splitting of 1.2 eV and a peak area ratio of 2 can be attained. In the freshly prepared Au/TiO$_2$ catalyst, the peaks for the S $2p_{3/2}$ and S $2p_{1/2}$ doublet (162.0 and 163.2 eV) can be assigned to the S−Au bond as reported in the literature.[21−23] Clearly, both thiol ends from DDT and MPA

(19) Xu, R.; Zeng, H. C. *Langmuir* **2004**, *20*, 9780−9790.
(20) Chang, Y.; Lye, M. L.; Zeng, H. C. *Langmuir* **2005**, *21*, 3746−3748.
(21) Lukkari, J.; Meretoja, M.; Kartio, I.; Laajalehto, K.; Rajamäki, M.; Lindström, M.; Kankare, J. *Langmuir* **1999**, *15*, 3529−3537.
(22) Gonella, G.; Cavalleri, O.; Terreni, S.; Cvetko, D.; Floreano, L.; Morgante, A.; Canepa, M.; Rolandi, R. *Surf. Sci.* **2004**, *566−568*, 638−643.
(23) Jiang, L.; Glidle, A.; McNeil, C. J.; Cooper, J. M. *Biosens. Bioelectron.* **1997**, *12*, 1143−1155.

molecules can contribute to the S−Au formation.[24] After 9 h of photoreactions using this catalyst, consistent with our FTIR results, it is found that both peaks show a significant decrease in intensity. It has been shown that the photolysis process can clean up alkanethiols from the Au surface by converting it to soluble alkyl sulfonate in solution.[23,25,26] After photoreaction, therefore, the removal of alkanethiols leads to weaker S 2p peaks compared with the freshly prepared catalyst.[22] This seems to support what we have predicted in the photoreactions: DDT molecules have been removed largely from the Au surface, while the majority of MPA is retained, considering the presence of Au nanoparticles. Besides the main doublets, there is another very weak one in both spectra (i.e., 163.3 eV for a and 163.0 eV for b). This component is doubtful or insignificant considering the noise level of the data, although the component has been explained to unbound thiol molecules or X-ray-induced molecular damage.[22,27] From curves c and d of the heat-treated catalysts, no S 2p peak in this BE range is found. This result is rather expected since all organic sulfur is oxidized away from the Au surface at a high temperature.

Figure 9 displays the XPS spectra of Ti 2p, which indicates that titanium in samples b−d has a chemical state of +4.[17] Note that the freshly prepared sample a shows a negative shift of 0.2 eV. This may be due to the existence of a large amount of surfactants that induces the congregation of electrons on the TiO_2 surface. The XPS peaks of Au $4f_{5/2}$ and $4f_{7/2}$, shown in Figure 10, for the nanosized metallic Au at 87.3 and 83.7 eV with a constant separation of spin−orbit coupling of 3.6 eV can be clearly observed for both the as-prepared and reacted catalysts. This result is consistent with our TEM results and S 2p XPS analysis. Since MPA is not expected to be removed during UV irradiation, Au can be bonded with TiO_2 through MPA linkers during the photoreaction. After heat treatment, however, Au 4f peaks show a negative shift of 0.2 eV (87.1 eV for $4f_{5/2}$ and 83.5 eV for $4f_{7/2}$; spin−orbit coupling separation = 3.6 eV). The observed shift has been related to the change of the Au particle size,[28−30] which is indeed observed in this study (Figure 6). We therefore attribute the observed shift to this size effect.[31] On the other hand, it is unsuspicious that the Au in the heat-treated catalysts (Figure 10; samples c and d) has a zero oxidation state (confirmed by 87.1 eV for $4f_{5/2}$ and 83.5 eV for $4f_{7/2}$) after thermal removal of MPA. But for the MPA-anchored samples a and b, relatively positive $Au^{\delta+}$ is expected since the electronegative element (sulfur) in the MPA can rip some electrons from Au particles.[10]

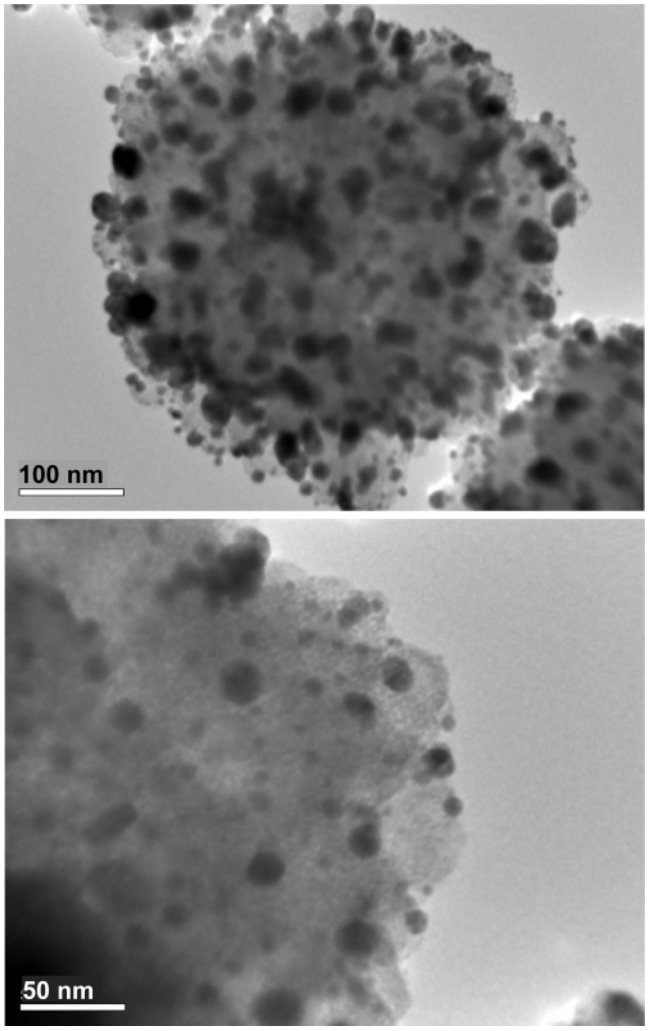

Figure 12. TEM images indicating that the particle size of Au nanoparticles deposited via a photoassisted method (route c, Figure 1) is much larger and less uniform. Experimental conditions: 2.0 mL of 0.040 M TiF_4 was added to 28.0 mL of H_2O and hydrothermally treated at 180 °C for 50 min (i.e., preparation of TiO_2 nanospheres). The prepared TiO_2 spheres were added with 0.04 mL of 0.010 M $HAuCl_4$ and 2.0 mL of PVP (0.05 g in 100 mL of H_2O). The mixture was then irradiated with the UV light for 1 h.

The O 1s XPS spectra exhibited in Figure 11 are quite complicated. All these spectra can be deconvoluted into four peaks with very similar BEs. The peak at 529.8 eV for samples b−d can be assigned to lattice oxygen in anatase TiO_2.[32] Compared to these samples, the freshly prepared one (a) has a negative shift at 529.5 eV, noting that the same kind of shift has also been observed in the Ti 2p spectra (Figure 10). It is believed that an abundant amount of surfactants such as DDT and TOAB in this sample is responsible for the negative shifts. The role of MPA must be trivial since it still exists in sample b, where no BE shift is observed. The two O 1s peaks at 533.2−533.4 and 531.5−531.7 eV in all these spectra can be assigned to oxygen species in H_2O molecules and Ti−OH or CO_3^{2-},[19,20] respectively, while the peak at 532.6−532.7 eV is attributed to

(24) Nakamura, T.; Kimura, R.; Sakai, H.; Abe, M.; Kondoh, H.; Ohta, T.; Matsumoto, M. *Appl. Surf. Sci.* **2002**, *202*, 241−251.
(25) Huang, J. Y.; Dahlgren, D. A.; Hemminger, J. C. *Langmuir* **1994**, *10*, 626−628.
(26) Behm, J. M.; Lykke, K. R.; Pellin, M. J.; Hemminger, J. C. *Langmuir* **1996**, *12*, 2121−2124.
(27) Castner, D. G.; Hinds, K.; Grainger, D. W. *Langmuir* **1996**, *12*, 5083−5086.
(28) Zhang, L.; Persaud, R.; Madey, T. E. *Phys. Rev. B* **1997**, *56*, 10549−10557.
(29) Chang, F.-W.; Yu, H.-Y.; Roselin, L. S.; Yang, H.-C. *Appl. Catal., A* **2005**, *290*, 138−147.
(30) Schumacher, B.; Plzak, V.; Kinne, M.; Behm, R. J. *Catal. Lett.* **2003**, *89*, 109−114.
(31) Zwijnenburg, A.; Goossens, A.; Sloof, W. G.; Crajé, M. W. J.; van der Kraan, A. M.; de Jongh, L. J.; Makkee, M.; Moulijn, J. A. *J. Phys. Chem. B* **2002**, *106*, 9853−9862.
(32) Centeno, M. A.; Paulis, M.; Montes, M.; Odriozola, J. A. *Appl. Catal., B* **2005**, *61*, 177−183.

C−OH or C−O−C groups from the oxidized carbon species of adventitious carbon (consistent with C 1s peak of 286.1 eV in Figure 7). It is also interesting to note that the TiO_2 surface of sample b is covered with more adsorbed species after photoreactions compared to that of sample a, based on a comparison of the relative intensity change of the lattice oxygen peaks of TiO_2 (Figure 11). In contrast, the TiO_2 surface becomes cleaner in the heat-treated sample (d) after similar photoreactions (compared with the sample (c)), on the basis of intensity changes observed in the peaks at 529.8 eV.

The above detailed information on the surface composition may shed light on our future design and fabrication of the self-assembled Au/TiO_2 catalysts. It should be pointed out that, in terms of controllability to generate monodisperse catalysts, the present self-assembly method is clearly more advantageous than other soft syntheses investigated in this work, although it is also important to recognize that monodisperse nanoparticles are not necessarily beneficial for all types of catalysis. In Figure 12, for example, the size of Au nanoparticles grown in a photoassisted synthesis (Figure 1c) is much less uniform compared to those prepared with the self-assembly method (see both Figure 1b and Figure 3), although the photoassisted on-site process can also be carried out at room temperature.

Finally, it should be mentioned that one of the unique features of the self-assembled catalysts is that the original active sites of the oxide support can be well-preserved, as there are plenty of unanchored areas of oxide supports in the resultant catalysts. In the conventional metal cation impregnation or photoassisted metal reduction, oxide supports have to be soaked in the metal salt solutions and ionic adsorption of metal species on the pristine oxide surface cannot be entirely avoided although sometimes this cationic adsorption/modification of oxide carrier may be beneficial. In contrast, the self-assembly method uses metal nanoparticle suspensions instead of metal salt solutions. As a new alternative illustrated in Figure 1b, apart from the loaded active metal nanoparticles, metal-free areas of the oxide carrier can be attained easily with the present self-assembly technique. These metal-free areas preserve intrinsic chemical functionality of the supporting oxide, ensuring the genuine composite nature for a desired materials system.

Conclusions

In summary, we have developed a self-assembly process to fabricate oxide-supported metal catalysts with a high monodispersivity for metal components. In these types of fabrications, presynthesized metallic nanoparticles, rather than on-site growing ones under thermally or photochemically activated conditions, can be "impregnated" evenly onto oxide supports with organic interconnects having bifunctional groups. Permanent engagement between the metal catalyst and oxide support can also be attained with simple heating. Methodic features of this technique have been demonstrated for Au/TiO_2 system in the photodegradation of methyl orange. In principle, other oxide-supported metal catalysts can also be fabricated at low temperatures through these types of self-assembling routes.

Acknowledgment. The authors gratefully acknowledge the financial support of the Ministry of Education, Singapore.

Supporting Information Available: EDX results (PDF). This material is available free of charge via the Internet at http://pubs.acs.org.

CM060362R